

Phenomenological analysis of domain width in rhombohedral BiFeO₃ films

C. W. Huang,¹ Lang Chen,^{1,*} J. Wang,¹ Q. He,² S. Y. Yang,² Y. H. Chu,³ and R. Ramesh²

¹*School of Materials Science and Engineering, Nanyang Technological University, 50 Nanyang Avenue, Singapore 639798, Singapore*

²*Department of Physics, University of California–Berkeley, Berkeley, California 94720, USA*

³*Department of Materials Science and Engineering, National Chiao Tung University, Hsinchu, Taiwan 30013, Republic of China*

(Received 10 August 2009; published 21 October 2009)

The experimental domain size scaling law in epitaxial BiFeO₃ films shows a different behavior from predictions of the conventional elastic domains: the (101)-type 71° domains are much wider than that of (100)-type 109° despite the larger domain-wall energy in (100) boundary. A phenomenological analysis for rhombohedral BiFeO₃ film is proposed, and it reveals that both the depolarizing energy and the elastic energy are indispensable for the equilibrium domain structures. With the increase in the asymmetrical electrostatic boundary on the film surfaces, the dominant domain scaling mechanism changes from electrostatic-dependent domain structure to elastic-dependent one, which is consistent with the experimental data. The present results highlight the general role of depolarizing field in rhombohedral domain structures.

DOI: [10.1103/PhysRevB.80.140101](https://doi.org/10.1103/PhysRevB.80.140101)

PACS number(s): 77.80.Dj, 77.22.Ej, 77.55.+f, 77.65.Ly

Ferroics break up into domain structures when cooled down through the Curie temperature T_c due to minimizing the total free energy.^{1–4} The ferroelectric domain structures are very sensitive to the electromechanical boundary conditions due to the long-range nature of their underlying electrostatic interaction on surfaces and to the strong coupling between the polarization and the strain on interface. Recently, the domain-dependent properties of rhombohedral BiFeO₃ film because of its potential applications with the high ferroelectric and antiferromagnetic temperature have been attracted intensive attentions.^{5–10} Experimentally, three possible polarization switching mechanisms, namely, ferroelastic 71° and 109° rotations, as well as ferroelectric 180° rotation have been observed.⁵

Domains of alternating polarization $\pm P$ are required for charge neutrality on the interfaces for the 180° ferroelectric domain structures.^{11–14} The electrostatic-dependent ferroelectric domain structures were investigated in tetragonal PbZr_{0.2}Ti_{0.8}O₃ thin film with or without electrodes systematically and showed that the depolarizing field does not affect the domain structure.¹⁵ On the other hand, the non-180° domains in constrained ferroelectric films are usually treated as elastic domains rather than ferroelectric ones on the assumption that the polarized charges on the surfaces can be compensated fully by the conductive oxide electrodes such as SrRuO₃ (SRO).^{16–19} The possible domain patterns may develop with either {100} or {101} boundaries in epitaxial rhombohedral ferroelectric films. Using the time-dependent thermodynamics such as phase field modeling in BiFeO₃ thin films,⁹ the substrate strain effects on the domain morphologies were shown that the domain structures could be controlled by choosing the proper substrate constraints. For the elastic-dependent BiFeO₃ thick films, the equilibrium do-

main width W as a function of film thickness D scales traditionally as $W \propto (\gamma D)^{1/2}$, which is proportional to the film thickness D and the domain-wall energy γ .^{7,16–20} However, there are few papers in discussion the depolarizing field effect on the rhombohedral BiFeO₃ film domain structures. The electrostatic boundary conditions need to be checked carefully in addition to elastic considerations. In fact, our experimental results show an opposite behavior against the pure elastic-dependent domain scaling law: the (101)-type 71° domains are much wider than that of (100)-type 109° despite the larger domain-wall energy in (100) boundary, whereas the domain-wall energy of $\gamma_{(100)}$ in rhombohedral BiFeO₃ is three times larger than that of $\gamma_{(101)}$ (Table I),²¹ which seems to be in contradiction according to the scaling law $W \propto (\gamma D)^{1/2}$.

The goal of this Rapid Communication is to investigate the effect of depolarizing field in BiFeO₃ films and propose a possible domain scaling law mechanism for the observational anomalous domain scaling law. The rhombohedral BiFeO₃ films ranging from 2 to 1000 nm were grown by pulsed laser deposition at 700 °C in an oxygen partial pressure of 100 mTorr on (001) SrTiO₃ (STO) substrate. A conducting SRO layer was used as a bottom electrode. The geometrical domain patterns are shown in Fig. 1 with the (001) planes aligned to the substrate. The 71° and 109° elastic domain walls correspond to the (101) and (100) boundaries, respectively. Piezoresponse force microscopy (PFM) has been widely used to analyze the ferroelectric polarization direction and domain structure in BFO films. The periodic ferroelectric domain was studied via PFM as shown in Fig. 2, which indicates that the size of 71° domain is larger than that of 109° domain.

The equilibrium domain structure and the relationship be-

TABLE I. Parameters of multiferroic BiFeO₃ film (Refs. 7, 9, and 22).

| P_{111} (C/m ²) | ν | G (GPa) | ϵ_a | $\gamma_{\{101\}}$ (J/m ²) | ω (deg) |
|----------------------------------|-------|--------------|--------------|---|-------------------|
| 1.0 | 0.35 | 69.0 | 200.0 | 0.09 | 0.6 |

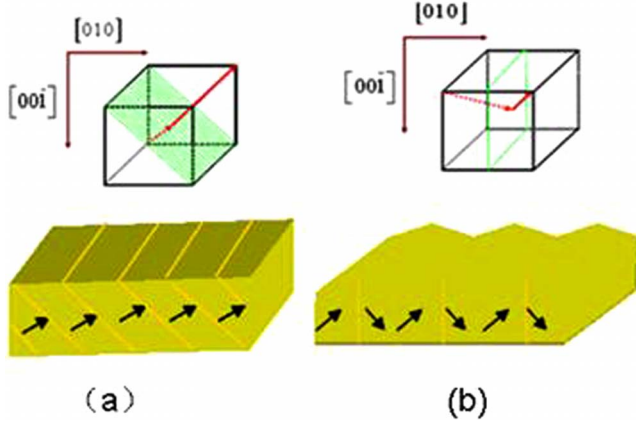


FIG. 1. (Color online) The domain-wall geometries of (100) and (101) boundaries in BiFeO₃ film; (a) (101)-type 71° domain and (b) (100)-type 109° domain.

tween the domain width W and the film thickness D can be obtained by minimizing the total energy of the ferroelectric system. The elastic energy F_e for (100) and (101) domain patterns can be expressed, respectively.¹⁸

For (101) domain pattern:

$$F_e = \frac{G\omega_s^2 W^2}{2\pi} \left[\frac{8D}{W} \tan^{-1} \frac{W}{2D} - \frac{4D}{W} \tan^{-1} \frac{W}{D} + \ln \left(\frac{4D^2 + W^2}{D^2 + W^2} \right) \right] + \frac{G\omega_s^2 D^2}{\pi} \ln \left[\frac{16D^3 \sqrt{D^2 + W^2}}{(4D^2 + W^2)^2} \right]. \quad (1)$$

For (100) domain pattern:



FIG. 2. (Color online) Large-area (5 $\mu\text{m} \times 5 \mu\text{m}$) PFM images of (001) grown; (a) 71° and (b) 109° periodic domain structure.

$$F_e = \frac{G\omega_s^2 W^2}{2\pi} \left[\frac{8D}{W} \tan^{-1} \frac{W}{2D} - \frac{4D}{W} \tan^{-1} \frac{W}{D} + \ln \left(\frac{4D^2 + W^2}{D^2 + W^2} \right) \right] + \frac{G\omega_s^2 D^2}{\pi} \ln \left[\frac{16D^3 \sqrt{D^2 + W^2}}{(4D^2 + W^2)^2} \right] + \frac{G\omega_d^2 D^2}{2\pi(1-\nu)} \ln \left(\frac{4D^2 + W^2}{D^2 + W^2} \right), \quad (2)$$

where G is the shear modulus, ω_s and ω_d are the magnitude of the shear ($\omega_s = \omega_d$), and ν is the Poisson's ratio.

Domains of alternating polarization $\pm P_0$ are distributed on the surfaces with the width W_+ and W_- in ferroelectric film, respectively. Lamina domains are characterized by the asymmetric electrostatic boundary condition $A [A = (W_+ - W_-)/(W_+ + W_-)]$ and changes from 0 to 1.0. Thus the expression of depolarizing field energy F_d is given by¹²

$$F_d = \frac{1}{2} \frac{p_0^2 D}{\epsilon_0 \epsilon_c} \left[A^2 + \frac{8g}{\pi^2 R} \sum_{n=1,2,\dots}^{\infty} \frac{1}{n^3} \sin^2 \left(n\pi \frac{A+1}{2} \right) \right] \times \frac{1}{1 + g \coth nR},$$

where

$$g = \sqrt{\epsilon_a \epsilon_c} (\epsilon_a = \epsilon_c), \quad R = \frac{\pi D}{2W} \sqrt{\frac{\epsilon_a}{\epsilon_c}}, \quad \text{and } P_0 = \frac{\sqrt{3}}{3} P_{111}. \quad (3)$$

The domain-wall energy can be written as $F_w = \gamma D/W$. The electrostatic boundary condition A can affect significantly the contribution of the electrostatic energy on the surfaces. First, for the symmetric neutral structure ($A=0$) in the BiFeO₃ film, the domain structure may develop with (100)-type 109° domain wall for the sake of mechanical and charge compatibility. The domain pattern is characterized by the parameters $W = W_+ = W_-$. Thus Eq. (3) can be simplified as

$$F_d = \frac{1}{2} \frac{p_0^2 D}{\epsilon_0 \epsilon_c} \left[\frac{8g}{\pi^2 R} \sum_{n=1,2,\dots}^{\infty} \frac{1}{n^3} \sin^2 \left(\frac{1}{2} n\pi \right) \frac{1}{1 + g \coth nR} \right]. \quad (4)$$

The equilibrium value W is determined by the energy minimum conditions. The thickness-dependent domain widths are shown in Fig. 3, taking into account the minimizations of different combinations of energy terms, e.g., $F_e + F_w$, $F_d + F_w$, and $F_e + F_d + F_w$.

For the thick BiFeO₃ films, the relationships between domain width W and film thickness D comply with the conventional rule with an exponent 0.5. However, all above classic domain scaling laws are predicted to collapse at small thickness. For the elastic domains the critical thickness $D_{crit} = 10\gamma/G\omega^2$ is about 390.0 nm.¹⁹ While for the ferroelectric domains the critical thickness $D_{crit} = 5\pi\gamma\epsilon_0\sqrt{\epsilon_c^3/\epsilon_a}/p_0^2$ is about 2.5 nm,¹² which is in accord with the experimental results that the ferroelectric phase is still stable for thickness down to 3 unit cell and the 180° stripe domains were ob-

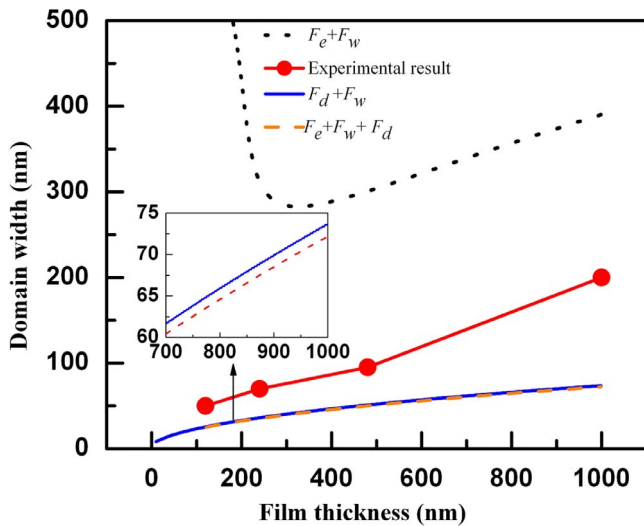


FIG. 3. (Color online) Theoretical and experimental results on the equilibrium domain width as a function of the film thickness with (100)-type 109° domain walls. The domain width increase significantly with a thin SRO compared to without SRO.

served for several nanometers in PbTiO_3 ultrathin films.²³ Meanwhile the domain width minimizing F_d+F_w is much less than the one from the elastic energy considering minimizing F_e+F_w , whereas the inset in Fig. 3 shows that the depolarized-dependent domain width F_d+F_w is slightly larger than that by minimizing $F_e+F_d+F_w$, which proves the vital role of the depolarizing energy in (100)-type BiFeO_3 domain patterns. The corresponding electrostatic-dependent domain scaling law is consistent with our experimental data compared with the elastic-dependent domain size (blank curve), which confirms the dominating role of the depolarizing field in (100)-type domain structure.

It was reported that the increase in miscut angle leads to the domain structures changing from multidomain (mixture of 109° and 71° domains) to single domain (71°) in BiFeO_3 film.¹⁰ The electric boundary condition A can also affect significantly the domain structures in the BiFeO_3 thin film. For a small A , the depolarized energy increases and the asymmetry of charges on the surface and consequently the width of domain increases. As A increases further, the domain structures change from 109° to 71° ones gradually. When $A=1$, there do not exist alternating polarization domains any more which may lead to a very large depolarizing energy $F_d = p_0^2 D / 2\epsilon_0 \epsilon_c$. The depolarizing charges on the film surfaces can be compensated completely with the existence of SRO conducting layers and result in the vanish of depolarizing energy. Thus, the theoretical thickness-dependent equilibrium domain structures are only determined by elastic energy and domain-wall energy and the domain structure may develop with (101)-type 71° domain walls at this condition in Fig. 4. In comparison, the experimental domain width scaling law is smaller than that of theoretical one and the magnitude of domain structure is impaired gradually with the reduction in film thickness.⁶ Although similar results have been studied by TEM on 4° miscut SrTiO_3 substrates, which induces a single 71° domain-wall structures,⁷ more attention should be paid to formula (1) in Ref. 7 due to the ambiguity

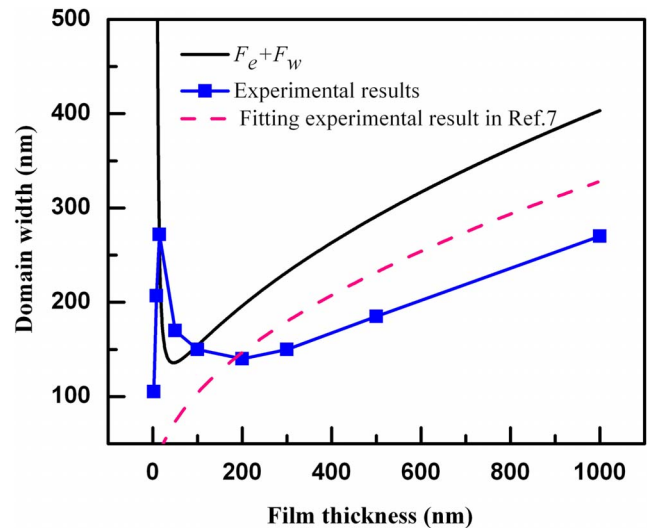


FIG. 4. (Color online) Theoretical and experimental results for the equilibrium domain width as a function of the film thickness with (101)-type 71° domain walls. Dash line was taken from Ref. 7.

between the shear strain G and Young's modulus E , which has a relevant relationship: $G = E / [2(1+\nu)]$. Therefore, the elastic-dependent theoretical result is larger than the experimental one in (101)-type BiFeO_3 film and the effect of depolarizing field is important and cannot be overlooked.

From the point of view of elastic energy, the domain width is relative to the domain-wall energy.¹⁸ The critical thickness for the 71° elastic domains is 130 nm, which is two thirds less than that of 109° ones due to the lower energy of 71° domain wall compared with that of 109° one.⁷ However, the experimental results in Fig. 5 revealed that the domain widths in 71° domain wall is sharply wider than that of 109° one for the same film thickness. Meanwhile, 71° domain walls are also observed larger compared to 109° domain walls by TEM,²⁴ which is qualitatively consistent with the "universal" proportionality between domain size and domain-wall thickness for all ferroics.²⁰ For 109° domain

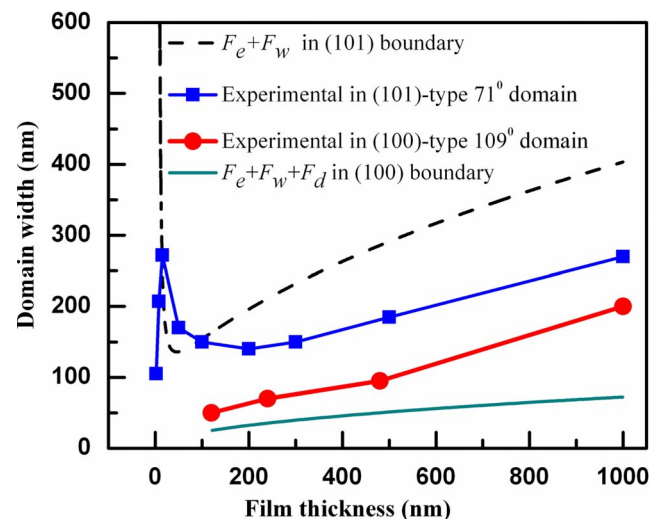


FIG. 5. (Color online) Comparison of the domain scaling laws in 71° and 109° domain walls.

wall, the equilibrium domain width is reduced greatly due to the effect of the depolarizing energy. As A increases, the electrostatic-dependent domain structures diminish gradually and the mechanism of the dominant domain scaling law changes from depolarizing dependent to elastic dependent. That is why that the domain width of 71° walls is obvious larger than that of 109° ones. Moreover, there is a gap between the theoretical and observational results on 71° domain scaling law. In many experimental works the domain structures were found far from neutrality ($0.5 < A < 1.0$) while the films are short circuit¹² that leads to the occurrence of 109° domain wall accompanying with depolarizing energy. In the present experiment, although the electrode (SRO) on the substrate neutralize mostly polarized charges on the interface between BFO/SRO, the depolarizing energy from the top surface still exist and compete against the elastic energy in the formation of equilibrium domain structures. In comparison the quantitative of the critical thickness and domain width with the experimental results in Fig. 5, it is indicated that the domain-wall energy, elastic energy, and depolarizing energy determine the equilibrium domain structures together on the epitaxial BFO/SRO/STO film regardless of the influence of miscut angle, and the 71° and 109° boundaries domain structures coexist and the popularity of 71° domain walls increase with electric boundary condition A . The similar experimental evolution of domain structure in LBFO thin film (substitution at Bi site with La, typically 10% La) has been studied but the observed result was attributed to the thickness-dependent transport properties of elec-

trode SRO thin film by using of OOP and IP PFM.²⁵ The depolarizing field decreases exponentially with the thickness of electrodes. Generally the depolarizing field vanishes with the thickness of the electrodes larger than 10 nm, this is why the BiFeO₃ film domain structures were investigated usually only from the point of view of elastic and domain-wall energies experimentally.⁶⁻⁸

In conclusion, we have investigated the domain structures and domain scaling law on the epitaxial BiFeO₃ film and found that (1) experimentally 71° domain is much wider than 109° domain, consistent with the proposed electrostatic-dependent theoretical results; (2) the domain structures change from (100)-type 109° domain walls to (101)-type 71° domain walls with the increase in electrostatic boundary condition A on the film surfaces; (3) the 71° and 109° domain walls coexist in thin BiFeO₃ film and the popularity of 71° domain walls increase with A even on the miscut substrate. More importantly, the influences of depolarizing field on the 71° and 109° domain structures discussed here can be applied for studying other rhombohedral domain structures such as BaTiO₃ and PbZr_{1-x}Ti_xO₃ ($0.06 < x < 0.47$).

The authors gratefully acknowledge the financial support from Nanyang Technological University under MoE Grants No. SUG 13/06, RG 21/07 and No. ARC 16/08; Y.H.C. would like to acknowledge the support of the National Science Council (R.O.C.) under Contract No. NSC98-2119-M-009-016.

*langchen@ntu.edu.sg

- ¹C. Kittel, Phys. Rev. **70**, 965 (1946).
- ²T. Mitsui and J. Furuichi, Phys. Rev. **90**, 193 (1953).
- ³A. L. Roytburd, Phys. Status Solidi A **37**, 329 (1976).
- ⁴G.-P. Zhao, L. Chen, and J. Wang, J. Appl. Phys. **105**, 061601 (2009).
- ⁵F. Zavaliche, S. Y. Yang, T. Zhao, Y. H. Chu, M. P. Cruz, C. B. Eom, and R. Ramesh, Phase Transitions **79**, 991 (2006).
- ⁶Y.-H. Chu, M. P. Cruz, C.-H. Yang, L. W. Martin, P.-L. Yang, J.-X. Zhang, K. Lee, P. Yu, L.-Q. Chen, and R. Ramesh, Adv. Mater. (Weinheim, Ger.) **19**, 2662 (2007).
- ⁷Y. B. Chen, M. B. Katz, X. Q. Pan, R. R. Das, D. M. Kim, S. H. Baek, and C. B. Eom, Appl. Phys. Lett. **90**, 072907 (2007).
- ⁸G. Catalan, H. Béa, S. Fusil, M. Bibes, P. Paruch, A. Barthélémy, and J. F. Scott, Phys. Rev. Lett. **100**, 027602 (2008).
- ⁹J. X. Zhang, Y. L. Li, S. Choudhury, L. Q. Chen, Y. H. Chu, F. Zavaliche, M. P. Cruz, R. Ramesh, and Q. X. Jia, J. Appl. Phys. **103**, 094111 (2008).
- ¹⁰H. Jang, D. Ortiz, S.-H. Baek, C. M. Folkman, R. R. Das, P. Shafer, Y. Chen, C. T. Nelson, X. Pan, R. Ramesh, and C.-B. Eom, Adv. Mater. (Weinheim, Ger.) **21**, 817 (2009).
- ¹¹Y. G. Wang, W. L. Zhong, and P. L. Zhang, Phys. Rev. B **51**, 5311 (1995).
- ¹²A. Kopal, T. Bahnik, and J. Fousek, Ferroelectrics **202**, 267 (1997).
- ¹³A. M. Bratkovsky and A. P. Levanyuk, Phys. Rev. Lett. **84**, 3177 (2000); **87**, 179703 (2001).
- ¹⁴S. K. Streiffer, J. A. Eastman, D. D. Fong, C. Thompson, A. Munkholm, M. V. Ramana Murty, O. Auciello, G. R. Bai, and G. B. Stephenson, Phys. Rev. Lett. **89**, 067601 (2002).
- ¹⁵S. P. Alpay, V. Nagarajan, L. A. Bendersky, M. D. Vaudin, S. Aggarwal, R. Ramesh, and A. L. Roytburd, J. Appl. Phys. **85**, 3271 (1999).
- ¹⁶W. Pompe, X. Gong, Z. Suo, and J. S. Speck, J. Appl. Phys. **74**, 6012 (1993).
- ¹⁷N. A. Pertsev and V. G. Koukhar, Phys. Rev. Lett. **84**, 3722 (2000).
- ¹⁸A. E. Romanov, M. J. Lefevre, J. S. Speck, W. Pompe, S. K. Streiffer, and C. M. Foster, J. Appl. Phys. **83**, 2754 (1998).
- ¹⁹N. Farag, M. Bobeth, W. Pompe, A. E. Romanov, and J. S. Speck, J. Appl. Phys. **97**, 113516 (2005).
- ²⁰G. Catalan, J. F. Scott, A. Schilling, and J. M. Gregg, J. Phys.: Condens. Matter **19**, 022201 (2007).
- ²¹C. A. Randall, D. J. Barber, and R. W. Whatmore, J. Mater. Sci. **22**, 925 (1987).
- ²²K. Yun, D. Ricinschi, T. Kanashima, and M. Okuyama, Appl. Phys. Lett. **89**, 192902 (2006).
- ²³D. D. Fong, G. B. Stephenson, S. K. Streiffer, J. A. Eastman, O. Auciello, P. H. Fuoss, and C. Thompson, Science **304**, 1650 (2004).
- ²⁴J. Seidel, L. W. Martin, Q. He, Q. Zhan, Y.-H. Chu, A. Rother, M. E. Hawkrige, P. Maksymovych, P. Yu, M. Gajek, N. Balke, S. V. Kalinin, S. Gemming, F. Wang, G. Catalan, J. F. Scott, N. A. Spaldin, J. Orenstein, and R. Ramesh, Nature Mater. **8**, 229 (2009).
- ²⁵Y.-H. Chu, Q. He, C.-H. Yang, P. Yu, L. W. Martin, P. Shafer, and R. Ramesh, Nano Lett. **9**, 1726 (2009).